FAILURE INITIATION DEPENDENCE ON SPECIMEN GEOMETRY IN OFF AXIS TESTS

C. Marotzke [1], T. Feldmann [2]

[1] BAM (Federal Institute for Materials Research & Testing), Division 5.3, Berlin, Germany, christian.marotzke@bam.de, www.bam.de
[2] BAM (Federal Institute for Materials Research & Testing), Division 5.2, Berlin, Germany, titus.feldmann@bam.de, www.bam.de

Keywords: Off axis test, Composites, Inter fiber failure, Stress concentrations, Anisotropic materials

ABSTRACT

The influence of the off axis angle and the length to width ratio on the stress field causing failure initiation in off axis tests is studied. The material under consideration is a carbon fiber reinforced epoxy resin. The elastic constants were determined experimentally by a series of off axis tests. The consequences of the coupling of all stress with all strain components encountered in anisotropic materials are outlined with respect to off axis tests. The stress and strain fields are analysed by means of finite element simulations. In particular the stresses arising in the critical zones at the edges where failure is initiated are evaluated. The change of the stress and strain fields depending on the off axis angle and the specimen geometry is analysed. The differences between ideal tensile tests and standard off axis tests are revealed.

1 INTRODUCTION

Off axis tests are used for the determination of the elastic constants as well as of the multiaxial strength of unidirectional plies. The fracture planes in unidirectional plies usually are parallel to the fibers because the inter fiber strength is much lower than the strength in fiber direction. Only in case of very low off axis angles fiber fracture occurs. The basic idea of off axis tests is to apply a deformation which is close to uniaxial tension. On the prospective fracture planes the ratio of normal to shear stresses is defined by the angle of the fracture plane, this is, by the off axis angle. In general, the determination of the elastic constants as well as the strength of a material necessarily requires a clearly defined stress and strain field at least in the region where the strain is measured or failure takes place, respectively. Preferentially a homogeneous stress and strain distribution is pursued. However, standard off axis tests are neither pure unidirectional tensile tests nor are the stresses and strains homogeneous. The deviation from ideal conditions is depending on the off axis angle and on the specimen geometry as a result of the anisotropy of the material.

A unidirectional ply is an orthotropic material if it is related to its natural coordinate system, this is, a coordinate system parallel to the axes of orthotropy. However, in any other coordinate system an orthotropic material behaves like a fully anisotropic material. Accordingly, a unidirectional ply loaded in axes not parallel to the axes of orthotropy deforms like a fully anisotropic material. In fully anisotropic materials stresses and strains are completely coupled. This means that axial strains give rise to shear stresses and, in turn, shear strains give rise to axial stresses. With respect to off axis tests this means that a pure axial stress requires a shear strain to develop in addition to the axial strain. Transverse strains, of course, do exist anyway. As a result of the complete coupling of stresses and strains, a pure tensile stress gives rise to a parallelogram like deformation. This deformation can be facilitated in off axis tests either by allowing a rotation of the clamps or a parallel shift of one clamp relative to the other. The shear deformation is by no means small. Depending on the off axis angle, the shear strain can even be higher than the average axial strain. A realisation of these deformations in practical tests would require special adaptions to standard testing machines which commonly are not available. Accordingly, most off axis tests are performed under non optimal conditions. In order to evaluate the reliability of the results achieved by standard test the grade of the deviations must be estimated. This is done in the present paper by analysing the stress and strain field arising in off axis

tests by means of finite element simulations by varying the off axis angle as well as the specimen geometry.

Off axis tests performed in standard testing machines which do not allow a rotation or a shift of the clamps undergo a complex deformation which, in turn, gives rise to a complex stress distribution. This was visualised by Pagano and Halpin [1] already in the late sixties on steel reinforced rubber under off axis loading showing that a kind of bending deformation together with shear is superposed to the tensile deformation. Strength measurements on composite plies under off axis loading were performed, among others, by Chamis and Sinclair [2]. Several aspects such as the determination of the shear modulus [3,4], the mechanical behaviour under compressive [5] and dynamic loading [6] were studied as well as general aspects of measuring the strength of composite plies [7, 8].

A general problem arising in mechanical tests which, as a matter of course, also is present in off axis tests is the load transfer from the clamps into the specimen. The clamping of the specimen results in a complex three-dimensional stress distribution in the clamped zones. In addition, the stress field in the vicinity is highly disturbed. In contrast to tensile specimens made of isotropic materials where the shape of the specimen can be adapted to reduce the intensity of the stress concentrations this is not possible in unidirectional plies. Even though tabs are mounted instead at the ends of the specimens in order to reduce the high stress concentrations at the edges of the clamps the stress field still is far from being homogeneous in these zones. A further factor which leads to a disturbance of the stress field is the constraint of the lateral contraction at the clamped ends. This results in substantial deviations from test conditions necessary to measure the true mechanical properties of the material instead of specimen dependent parameters.

A detailed investigation of the stress field in the load transfer zones close to the clamps is very extensive. It is depending on several parameters such as the shape of the glue at the edges of the tabs as well as its adhesive properties. This is outside the scope of this paper and left to a further analysis. Here, the problem of the load transmission is simplified by applying displacement boundary conditions directly at the ends of the specimen. As a result of these simplifications the stresses and strains in the direct vicinity of the boundaries are not taken into account in the evaluation because the present model is not appropriate to give reliable data in these zones.

2 OFF AXIS TEST SPECIMEN - FINITE ELEMENT MODEL

The standard specimen used for the series of off axis experiments performed in order to determine the elastic constants and strength has a length of 70 mm and a width of 12 mm giving a length to width ratio of 5.8 (table 1). Since for low off axis angles no pure inter fiber failure can take place because no crack connecting the free edges can develop a second type of specimen is used in the practical tests with a larger length to width ratio. Since the width cannot be reduced significantly because the strain gauges need some space the length of the specimens is increased to 280 mm giving a length to width ratio of 23.3. For the finite element simulations both alternatives are equivalent as long as the fineness of the mesh is adapted. For practical reasons specimens having the same length (70 mm) but different widths are used for the present simulations giving the respective length to width ratios. The 280 mm specimen accordingly is replaced by a 70 mm specimen with a width of 3 mm (table 1).

Length L (mm)	Width B (mm)	Length to Width ratio (L/B)	Application
70	12	5.8	Tests / FEM
70	3	23.3	FEM
280	12	23.3	Tests

Table 1: Specimen geometry

The material under investigation is a carbon fiber reinforced epoxy resin with a fiber volume fraction of 55%. The engineering constants given in table 2 are experimentally determined in a series

of off axis tests by varying the off axis angles between 0° and 90°. The axial strain is measured by strain gauges fixed in the middle of the specimens. The shear modulus is back calculated from the elastic moduli as being functions of the off axis angles. This method is preferred to explicit shear tests using a shear frame because the accuracy of the shear modulus is in the same range while saving experimental effort as well as testing material. Standard 8-node plane stress elements are used in the finite element simulations. The loading is applied via prescribed displacements at one end while fixing the other end. The transverse displacements are fixed at both ends which represents a strong idealisations of the true clamping conditions. The material is modelled as a linear elastic orthotropic material presuming small deformations.

Engineering constants	Value	
E_1	113300	MPa
E_2	7960	MPa
G_{12}	4000	MPa
ν_{12}	0.32	-

Table 2: Engineering constants of CFRP specimen

In order to get a basic insight into the deformation behaviour of orthotropic materials under off axis loading the interaction of shear and normal stresses with the respective strains is studied. The interaction is governed by the stiffness coefficients given in the global coordinate system which are derived from the orthotropic coefficients using standard transformation rules. For the material under consideration the dependence of the stiffness coefficients on the off axis angles is shown in fig. 1a.

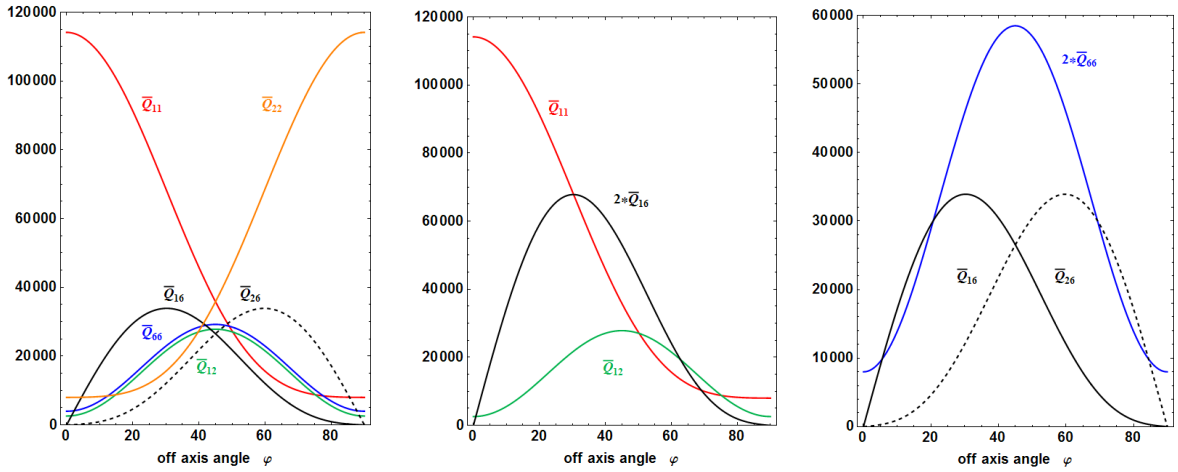

Figure 1: Stiffness coefficients versus off axis angle a) stiffness coefficients b) coefficients governing the axial stresses c) coefficients governing the shear stresses

In order to ease the estimation of the influence of the respective strains the effective coefficients are plotted in figs. 1b and 1c. Referring to the constitutive equations the effective coefficients are the shear strain related stiffness coefficients multiplied by a factor of two. The coefficients governing the axial stresses (1.1) are given in figure 1b. The axial stresses depend on the axial strains ε_{xx} via $\overline{Q}_{11}$, on the shear strains ε_{xy} via $2*\overline{Q}_{16}$ and on the transverse strains ε_{yy} via $\overline{Q}_{12}$. The course of $\overline{Q}_{11}$ shows that the axial stresses at low off axis angles are dominated by the axial strains, as expected. The influence of the shear strains however grows very rapidly leading to a dominance for off axis angles greater than

30°, as indicated by the course of $2*\overline{Q}_{16}$. This means that for a wide range of angles the axial stresses are stronger dependent on the shear than on the axial strains. At angles above 40° even the transverse strains get a major influence. Between 40° and 70° all three coefficients are close together. Around 60° transverse and shear strains have a higher influence on the axial stresses than the axial strains themselves. This reveals how different anisotropic materials behave compared to isotropic ones.

$$\sigma_{xx} = \overline{Q}_{11}\,\varepsilon_{xx} + \overline{Q}_{12}\,\varepsilon_{yy} + 2\overline{Q}_{16}\,\varepsilon_{xy} \tag{1.1}$$

$$\sigma_{yy} = \overline{Q}_{12}\,\varepsilon_{xx} + \overline{Q}_{22}\,\varepsilon_{yy} + 2\overline{Q}_{26}\,\varepsilon_{xy} \tag{1.2}$$

$$\sigma_{xy} = \overline{Q}_{16}\,\varepsilon_{xx} + \overline{Q}_{26}\,\varepsilon_{yy} + 2\overline{Q}_{66}\,\varepsilon_{xy} \tag{1.3}$$

The shear stresses (1.3) depend on the shear strains via $2*\overline{Q}_{66}$, on the axial strains via $\overline{Q}_{16}$ and on the transverse strains via $\overline{Q}_{26}$ (fig. 1c). For better visibility the scale in figure 1c is enlarged by a factor of two. Between 5° and 20° the shear stresses depend on shear and axial strains almost on equal share. For angles below 5° and above 85° as well as between 20° and 70° the shear strains are the dominating part. Since $\overline{Q}_{16}$ and $\overline{Q}_{26}$ are antisymmetric to each other the contribution of axial and transverse strains to the shear stresses is interchanged.

These results show that the dependence of the stresses on the strain components strongly varies with the off axis angle. This, in turn, means that also the strain field itself, strongly changes with the off axis angle. As a result, the complete failure behaviour arising in off axis specimens is highly influenced by the off axis angle.

A rough insight into the complex deformation taking place in off axis specimens can be achieved by splitting the deformation in two steps. In the first step a pure tensile stress is applied resulting in a parallelogram like deformation realised by a transverse shift of one end (fig. 2a). In a second step the end is shifted back by applying a transverse displacement on the primarily free end. The shifting by simultaneously fixing the rotation of the ends results in a kind of double bending deformation superposed by an additional shear deformation (fig. 2b). The high shear deformation becomes obvious in particular near the clamped ends. The deformed specimen (fig. 2b) has a principal similarity with the experiments of Pagano and Halpin [1]. However, the material under investigation is linear elastic giving rise to small deformations. In figures 2a and 2b the deformations are graphically enhanced and do not allow a direct comparison with the experimental results. They rather show the general trend.

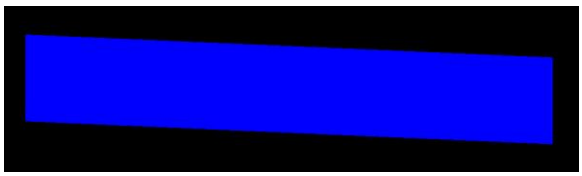

Figure 2a: Axial stresses in 15° off axis specimen free shear shear deformation

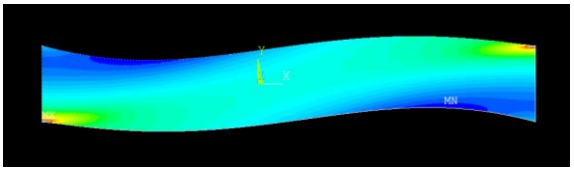

Figure 2b: Axial stresses in 15° off axis specimen shear deformation constrained at the ends

3 STRAIN DISTRIBUTION DEPENDING ON OFF AXIS ANGLE

Some general features of the stress and strain field arising in off axis tests were studied in [10] for a specific off axis angle (15°). Since the stress and strain field is strongly depending on the off axis angle, especially at lower angles, in the present paper the angles are varied between 6° and 45°. In addition the influence of the length to width ratio is analysed for these angles (table 1). In off axis tests the highest stresses arise at the edges close to the clamps or, at least, in the direct vicinity. As they are governing the failure initiation the study focusses on them. Since the stresses and strains are antisymmetric to the middle plane (y=0) only one edge (lower edge) is analysed. The stress and strain fields are evaluated at off axis angles of 6°, 15°, 30° and 45°.

In order to compare the specific dependencies of the three strain components on the off axis angle as well as on the geometry the same average strain is applied for any off axis angle and both length to width ratios. First, some basic characteristics of off axis tests are addressed. Independent of the type of material shear stresses σ_{xy} as well as transverse stresses σ_{yy} have to vanish at free edges as result of the equilibrium conditions. Similar to tensile tests of isotropic materials the axial stresses at the edges can be given as a function of the axial strains only. In tensile tests of isotropic materials the transverse stresses σ_{yy}, σ_{zz} vanish while shear stresses are absent a priori owing to the material law. As a result the transverse strains ε_{yy}, ε_{zz} can be eliminated and substituted by ε_{xx}. In off axis tests, on the other hand, plane stress conditions are fulfilled a priori. However, the stresses are still depending on three strain components, this is, on the axial ε_{xx} and transverse strains ε_{yy} and, in addition, on the shear strains ε_{xy}. Accordingly, the shear and transverse strains can be substituted by the axial strains ε_{xx} here. As a result the axial stresses σ_{xx} at the edges can be written as a function of the axial strains only with the axial E-modulus of the ply as proportionality factor. It has to be mentioned that this condition is strictly fulfilled only at the edges. Of course, it also has some influence on the neighbourhood. Moving towards the center the courses of the respective strains becomes different more and more, especially near the clamped ends. This is another indication for the strong influence of the clamping conditions on the stress and strain field..

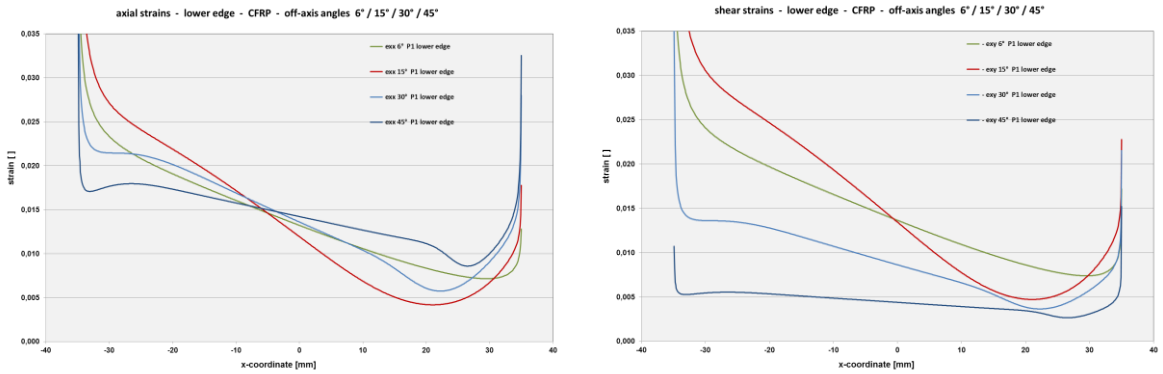

a) axial strains ε_{xx} b) shear strains ε_{xy}

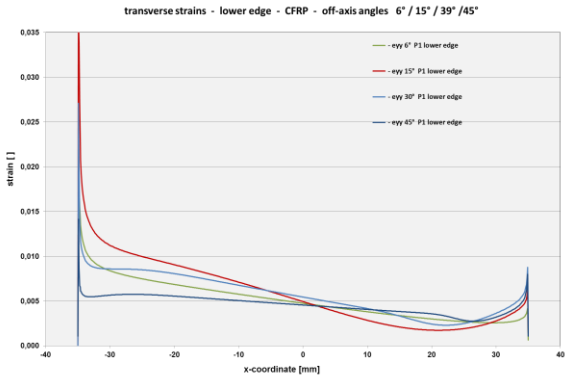

c) transverse strains ε_{yy}

Figure 3: Dependence of strains at lower edge on off axis angle

The axial strains at the lower edge for the respective off axis angles are given in fig. 3a. Near the ends the strains are very high for any angle. The high level of the strains is a result of the singularity arising at the corner which will be addressed later on. The general increase towards the ends is caused

by the constrained shear deformation due to the clamping and, to a minor extend, by fixing the lateral contraction. In the middle of the specimen the course of the strains is rather linear. The highest slope arises in case of the 15° off axis specimen. For higher angles the axial strains exhibit a slight minimum close to the ends followed be an extreme increase. It has to be mentioned that the average of the axial strains does not change with the off axis angle as it is prescribed by the boundary conditions.

The level of the shear strains at the edge is strongly dependent on the off axis angle (fig. 3b). While for angles of 6° and 15° the averages of the shear strains do not differ very much they decrease significantly for the higher angles. The course of the axial and shear strains indicates that a kind of bending together with a remarkable shear deformation takes place, as visualised by Pagano [1]. The average of the transverse strains, on the other hand, only slightly varies with the off axis angle (fig. 3c). Close to the left end the transverse strains exhibit a very strong increase. Directly at the end it falls to zero because the lateral contraction is constrained by the boundary conditions here.

The course of the three strain components shows that with growing off axis angle the axial strains become more and more dominant. For an off axis angle of 45° the axial strains are more than three times the shear strains. This is not surprising because with the off axis angle approaching 90° the material behaviour approximates more and more the orthotropic state. That is, the constraining of the shear deformation by the clamps becomes increasingly irrelevant.

4 STRAIN DISTRIBUTION DEPENDING ON THE SPECIMEN GEOMETRY

The influence of the length to width ratio on the stress and strain distribution is studied by comparing two ratios differing by a factor of four. The variation of the length to width ratio has some relevance for practical tests with respect to strength measurements at small off axis angles. Here, a high length to width ratio is needed in order to facilitate pure inter fiber failure. In addition to showing the influence of the geometry the following diagrams allow a direct comparison of the axial and shear strains for each angle.

For a 6° off axis specimen the axial as well as the shear strains are almost identical showing a largely linear decay in the middle of the specimen and a strongly nonlinear increase towards the ends (fig. 4a). The full lines correspond to a length to width ratio of 5.8 while the dotted lines to a four times higher ratio of 23.3. The specimen with the large length to width ratio reveals the same trend, however the slope in the middle part is much smaller. That means that the slender specimen suffers less bending and shear deformation revealing that it is closer to the deformation of an actual tensile test. In addition, the extension of the zone of nonlinearity is smaller but, at the same time, the increase is much steeper. The steep increase in the direct vicinity of the ends sharpens the problem of the reliability of the calculated stresses close to the ends.

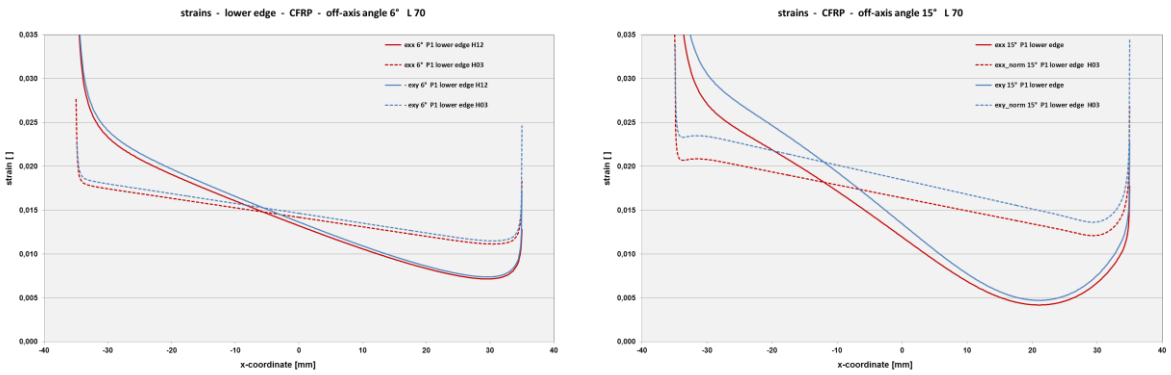

a) off axis angle 6° b) off axis angle 15°

Figure 4: Dependence of the strains on the length to width ratio; full lines: length to width ratio 5.8 dotted lines: length to width ratio 23.3

The change of the length to width ratio for a 15° specimen also leads to a reduction of the slope of the respective strains (fig. 4b). According to the boundary conditions the average of the axial strain is

independent of the off axis angle and of the length to width ratio as well. As a consequence of this condition it can be concluded from the coupling of the strains at the edges (see section 3) that also the average of the shear strains must be the same for both ratios. Accordingly the course of the shear strains changes with variation of the length to width ratio but the average value does not. With further growth of the off axis angle (30°, 45°) the slope of the axial and the shear strains is further decreased for the higher length to width ratio (fig. 5a, 5b). The minimum of the shear strains close to the right end becomes more and more pronounced.

In any case the slender specimens offer a strain distribution which is closer to a pure tesile test. The bending and shearing is signicantly reduced. The problem of the disturbance near the clamped zones is reduced, however, still it is not negligible.

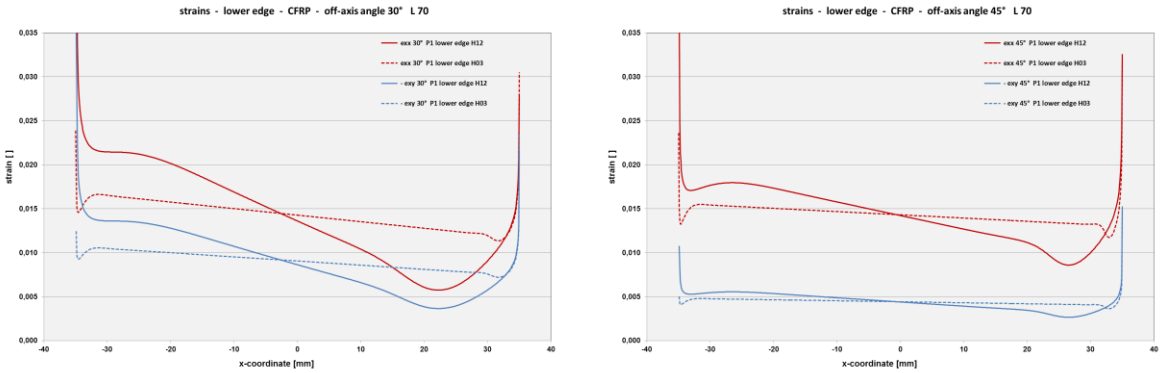

a) off axis angle 30° b) off axis angle 45°

Figure 5: Dependence of strains on length to width ratio; full lines: length to width ratio L/B=5.8; dotted lines: length to width ratio L/B=23.3

5 STRESS FIELD INSIDE SPECIMEN

The finite element analyses based on the present model show that the maximum axial stresses arise at the corners where the edges meet the fixed boundaries. As mentioned above the stresses in the direct vicinity of the corners are strongly disturbed as a result of the clamps and, in particular, by the stress singularity (see below) and cannot be predicted with the same accuracy as the stresses in the remaining part of the specimen. Accordingly failure may occur anywhere in the surrounding zone, depending on local faults in the specimen. In order to get an estimation of the stress field inside the specimen the axial stresses at several positions across the specimen width are studied for an off axis angle of 15°. For sake of improving the visibility the stresses are given in two separate figures. The stresses in the lower half are shown in fig. 6a for the full specimen length. The stresses over the full cross section for the left half of the specimen are shown in fig. 6b.

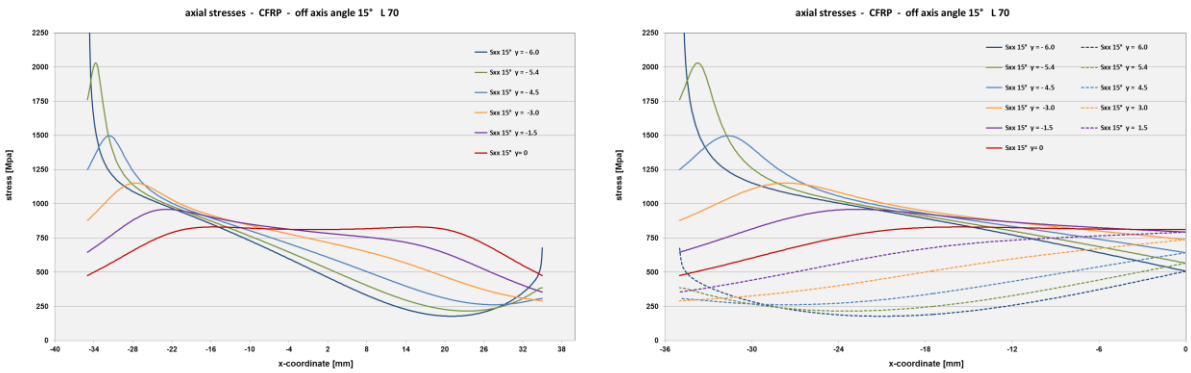

a) lower half, full specimen length b) full cross section, left half of specimen

Figure 6: Axial stresses at various distances from center line

Besides the lower edge the axial stresses at further lines located at 90%, 75%, 50% and 25% of the half width are evaluated. The specimen under investigation has a length of 70 mm and a width of 12 mm. That is, the 90% line (green line) has a distance of 0.54 mm from the edge, the 75% line 1.5 mm (blue line), the 50% line 3.0 mm (yellow) and the 25% line 4.5 mm (violet line). In addition, the stresses at the center line are given (red line).

First, the axial stresses in the lower half are studied. At the lower edge the stresses (dark blue line) show a steep increase towards the fixed end (fig. 6a) leading to a very high maximum which indeed is outside the scale. At the corner the stress value predicted by the numerical solution is not reliable because a stress singularity exists at this point within the theory of elasticity. At a singularity the level of the calculated stresses is highly depending on the mesh fineness and in so far arbitrary. Inside the specimen the maxima arise in some distance from the boundary. The distance grows when moving towards the center line. At the same time the maxima decrease and the stress distributions become more uniform. The stresses directly at the boundary also decrease and are below the average axial stresses of the specimen. This tendency first continues also in the upper half (fig. 6b, dotted lines). Close to the upper edge the stresses increase again. This is due to a further stress singularity existing at the corner of the upper edge. However, the stress intensity at the upper corner is significantly lower compared to the lower corner. The distribution of the axial stresses is highly inhomogeneous, only near the center (x=0, y=0) the stresses are relatively homogeneous. The other stress components play a minor role. The shear stresses are about one order of magnitude lower than the axial stresses while the transverse stresses are almost vanishing.

From the stress field predicted by the present model failure is most likely to occur in the immediate surrounding of the corners, this is, the lower left or the upper right corner. Experiments show that indeed in several cases failure occurs in these zones but also in many cases fracture takes place outside the direct vicinity of the corners. Obviously the stress distributions based on the two-dimensional model do not completely reflect the actual stresses responsible for failure initiation. On one hand this is because the stresses in the critical zone close to the clamps cannot be predicted with a sufficient accuracy by the two-dimensional model under consideration. In addition, further factors have substantial influence on the location of failure initiation as well as on the level of the external loading. There is, for example, the machining of the specimens which causes some local damage at the edges. Furthermore the material itself has some local variations of the mechanical properties, e.g. the fiber volume fraction varies locally and faults in the matrix or in the interfaces between fibers and matrix may exist.

7 CONCLUSIONS

The study confirms that failure is most likely to occur at the edges of the specimens close to the clamped ends. The disturbance of the stress and strain fields due to the constrained shear deformation and, in addition, due to the prevented lateral contraction has wide ranging consequences on the stress distribution. A large length to width ratio leads to a more uniform stress and strain field, especially in the middle part of the specimens. However, high stress and strain concentrations near the ends are still present. As a result, a more detailed analysis of the regions near the clamps using a three-dimensional model is required for improving the reliability of the prediction of failure initiation.

ACKNOWLEDGEMENTS

The authors would like to thank Lothar Buchta (BAM) and Fabian Roth (BAM) for specimen preparation and performance of the tests.

REFERENCES

[1] N. J. Pagano, J. C. Halpin, Influence of end constraint in the testing of anisotropic bodies, *Journal of Composite Materials*, **2**, 1968, pp. 18-31

[2] J. H. Sinclair, C. C. Chamis, Fracture modes in off-axis fiber composites, *Polymer Composites*, **2**, 1981, pp. 45-52

[3] J. C. Marin, J. Canas, F. Paris, J. Morton, Determination of G12 by means of the off-axis tension test, Part I, *Composites Part A*, **33**, 2002, pp. 87-100

[4] J. C. Marin, J. Canas, F. Paris, J. Morton, Determination of G12 by means of the off-axis tension test, Part II, *Composites Part A*, **33**, 2002, pp. 101-111

[5] Q. Bing, C. T. Sun, Specimen size effects in off-axis compression tests of fiber composites, *Composites Part B*, **39**, 2008, pp. 20-26

[6] L. Ninan, J. Tsai, C. T. Sun, Use of split Hopkinson pressure bar for testing off-axis composites, *International Journal of Impact Engineering*, **25**, 2001, pp. 291-313

[7] C. Marotzke, T. Feldmann, Failure processes of fiber reinforced composites under off axis loading, *Proc. Of ICCM20*, Copenhagen, 2015

[8] A. Puck, H. Schürmann, Failure analysis of FRP laminates by means of physically based phenomenological models, *Composites Science and Technology*, **62**, 2002, pp. 1633-1662